JOURNAL OF VIROLOGY, May 1989, p. 2169–2179
0022-538X/89/052169-11$02.00/0

Vol. 63, No. 5

Physical Mapping and Nucleotide Sequence of a Herpes Simplex Virus Type 1 Gene Required for Capsid Assembly

B. PERTUISET,[1] M. BOCCARA,[1†] J. CEBRIAN,[1] N. BERTHELOT,[1] S. CHOUSTERMAN,[1‡] F. PUVION-DUTILLEUL,[1] J. SISMAN,[2] AND P. SHELDRICK[1*]

Institut de Recherches Scientifiques sur le Cancer, 94802 Villejuif Cédex,[1] and Institut Pasteur, 75015 Paris,[2] France

Received 28 June 1988/Accepted 13 January 1989

In this report, we describe some phenotypic properties of a temperature-sensitive mutant of herpes simplex type 1 (HSV-1) and present data concerning the physical location and nucleotide sequence of the genomic region harboring the mutation. The effect of shifts from the permissive to the nonpermissive temperature on infectious virus production by the mutant A44ts2 indicated that the mutated function is necessary throughout, or late in, the growth cycle. At the nonpermissive temperature, no major differences were detected in viral DNA or protein synthesis with respect to the parent A44ts$^+$. On the other hand, electron microscopy of mutant-infected cells revealed that neither viral capsids nor capsid-related structures were assembled at the nonpermissive temperature. Additional analyses employing the Hirt extraction procedure showed that A44ts2 is also unable to mature replicated viral DNA into unit-length molecules under nonpermissive conditions. The results of marker rescue experiments with intact A44ts2 DNA and cloned restriction fragments of A44ts$^+$ placed the lesion in the coordinate interval 0.553 to 0.565 (1,837 base pairs in region U_L) of the HSV-1 physical map. No function has previously been assigned to this region, although it is known to be transcribed into two 5′ coterminal mRNAs which code in vitro for a 54,000-molecular-weight polypeptide (K. P. Anderson, R. J. Frink, G. B. Devi, B. H. Gaylord, R. H. Costa, and E. K. Wagner, J. Virol. 37:1011–1027, 1981). We sequenced the interval 0.551 to 0.565 and found an open reading frame (ORF) for a 50,175-molecular-weight polypeptide. The predicted product of this ORF exhibits strong homology with the product of varicella-zoster virus ORF20 and lower, but significant, homology with the product of Epstein-Barr virus BORF1. For the three viruses, the corresponding ORFs lie just upstream of the gene coding for the large subunit of viral ribonucleotide reductase. The ORF described here corresponds to the ORF designated UL38 in the recently published nucleotide sequence of the HSV-1 U_L region (D. J. McGeoch, M. A. Dalrymple, A. J. Davison, A. Dolan, M. C. Frame, D. McNab, L. J. Perry, J. E. Scott, and P. Taylor, J. Gen. Virol. 69:1531–1574, 1988).

In the nucleus of the herpesvirus-infected cell, viral DNA and several virus-specified proteins are assembled into nucleocapsids that subsequently acquire composite protein-lipid envelopes as they leave the nucleus and migrate to the exterior of the cell. The chain of events leading to the formation of nucleocapsids is incompletely understood, although there is suggestive evidence that one of the steps involves the packaging of viral DNA into performed capsids (reviewed in references 7 and 67). A frequent observation taken in support of this is that capsid assembly still occurs, albeit at reduced efficiency, when DNA synthesis is prevented either by chemical means (22, 51, 56) or by growth under nonpermissive conditions for various temperature-sensitive (*ts*) mutants (4, 7, 9, 13, 59). In fact, the great majority of all herpesvirus *ts* mutants for which this aspect of the phenotype has been studied are apparently able to assemble some form of capsidlike structure, whether empty, partial cored, or aberrant, during nonpermissive growth (1, 4, 6, 7, 9, 13, 35, 52, 59, 63, 70).

The capsid-negative phenotype, in which no capsid-related structures are produced at all, has been observed among *ts* mutants of herpes simplex virus type 1 (HSV-1) (13, 59,70), HSV type 2 (HSV-2) (4, 9), and pseudorabies virus (PrV) (7, 35, 36). Certain *ts* capsid-negative mutants affect capsid assembly by grossly interfering with viral gene expression. These mutants produce a thermolabile immediate-early regulatory protein (175K/ICP4 for HSV-1 [13, 18]; 180K IE for PrV [7]) and are blocked for the subsequent synthesis of all early and late viral gene products, as well as for viral DNA replication. Others, however, appear to interfere with the capsid assembly pathway in a more direct way. These mutants express most, if not all, viral proteins at normal levels throughout the infectious cycle and replicate viral DNA. Thus far, such DNA-positive capsid-negative *ts* mutants have been assigned to a single complementation group in both HSV-1 and HSV-2 (60) and to two or three complementation groups in PrV (36). For HSV-1, the relevant complementation group, 1-7, has been mapped to the gene for the 155,000-molecular-weight major capsid protein in the coordinate interval 0.235 to 0.271 of the genome (70).

Here we describe a *ts* mutant, A44ts2, of HSV-1 which also displays the DNA-positive capsid-negative phenotype but whose mutation maps by marker rescue to the coordinate interval 0.553 to 0.565. The nucleotide sequence of this region as determined in this work, and independently by McGeoch et al. (42), contains an open reading frame (ORF) for a 50,000-molecular-weight protein previously identified as a 54,000-molecular-weight product of in vitro-translated HSV-1 RNA (2).

(A preliminary account of the marker rescue and nucleotide-sequencing portions of this work was presented at the 11th International Herpesvirus Workshop, Leeds, England, in July 1986.)

* Corresponding author.
† Present address: Laboratoire de Pathologie Végétale I.N.A., 75005 Paris, France.
‡ Present address: Unité 245, Centre INSERM Saint Antoine 184, 75751 Paris, France.

MATERIALS AND METHODS

Cells and viruses. The RS537 line of rabbit skin fibroblasts (61) used throughout this work was propagated in Eagle minimal essential medium (MEM) supplemented with 5% fetal calf serum in the absence of antibiotics. High-titered stocks of the parental strain A44ts$^+$ were prepared after infection at 37°C in MEM–2% fetal calf serum as described previously (61). Stocks of the mutant A44ts2 were prepared following growth at 30°C.

Plaque titration of virus was performed on cell monolayers in 60-mm plastic petri dishes overlaid with MEM–2% fetal calf serum containing 0.6% carboxymethyl cellulose. Incubation in an atmosphere of 95% air–5% CO_2 was at 37°C for A44ts$^+$ and 30°C for A44ts2. Plaques were developed by treatment of the monolayer with 0.05% neutral red in phosphate-buffered saline (PBS).

Mutagenesis and screening for *ts* mutants. Confluent monolayers were infected with A44ts$^+$ at 10 PFU per cell and incubated at 34°C for 4 h. The medium was replaced with PBS containing *N*-methyl-*N'*-nitro-*N*-nitrosoguanidine (Aldrich Chemical Co., Inc., Milwaukee, Wis.) at a concentration of 1 mg/ml, and incubation was continued at 34°C for 30 min. After removal of the mutagen and several rinses with PBS, fresh medium was added and the monolayers were incubated for 48 h at 30°C. Final yields of infectious virus were reduced by a factor of 10^4 in mutagen-treated cultures as compared with PBS-treated controls. Dilutions of mutagenized stocks were used to infect cell monolayers in microdilution wells (Falcon Microtest) at 30°C such that 50 to 75% of the wells showed advanced cytopathic effects after several days. The contents of the wells were then transferred to duplicate microdilution plates with a replica plating device as described by Robb and Martin (57) for incubation at 38°C.

Single-cycle virus growth and temperature shift experiments. Confluent cell monolayers in 60-mm plastic petri dishes (2×10^6 cells per dish) were infected at a multiplicity of 10 PFU per cell in 1 ml of MEM at 37°C for 30 min. Following two washes with MEM, the dishes were flooded with 2 ml of MEM–2% fetal calf serum (taken as $t = 0$) and incubated at 30 or 38°C for the desired times. Cultures were plaque titrated after three freeze-thaw cycles followed by clarification by low-speed centrifugation.

Viral DNA extraction. Stocks of CsCl-purified virus (61) were lysed with 1% (final concentration) sodium dodecyl sulfate in the presence of 10 mM EDTA and extracted three times with equal volumes of phenol preequilibrated with 100 mM Tris hydrochloride (pH 8). DNA to be used in transfection experiments was exhaustively dialyzed against 10 mM Tris hydrochloride (pH 7.5)–1 mM EDTA, and its infectivity was assayed as described below. For cloning, DNA was further purified by sedimentation through 5 to 20% sucrose gradients as previously described (61).

Radiolabeling and buoyant density centrifugation of infected cell DNA. Monolayers infected at 38°C with 10 PFU per cell were labeled with [^{3}H]thymidine at 5 μCi/ml from 6 to 9 h postinfection. After freezing (−70°C) and thawing, pronase (50 μg/ml) in 100 mM NaCl–10 mM Tris hydrochloride (pH 7.2)–10 mM EDTA–0.5% sodium dodecyl sulfate was added (2 ml/60-mm dish) for 30 min at 37°C. The lysates were adjusted to a density of 1.71 g/cm^2 with CsCl and centrifuged in a Beckman SW50 rotor at 40,000 rpm for 60 h at 20°C. Fractions were collected for determination of refractive index and, following trichloroacetic acid precipitation, determination of radioactivity.

Radiolabeling and polyacrylamide gel electrophoresis of infected cell polypeptides. Infected monolayers at 37°C in MEM lacking methionine (30-mm dishes, 5×10^5 cells per dish) were labeled with 100 μCi of [^{35}S]methionine per ml from 22 to 24 h postinfection. Cells were harvested by scraping and washed by centrifugation at low speed in PBS, and the final pellet was suspended directly in sample application buffer (60 mM Tris hydrochloride [pH 6.8], 2% sodium dodecyl sulfate, 5% 2-mercaptoethanol, 10% glycerol) (37). Electrophoresis was done on 10% (wt/wt) polyacrylamide gels cross-linked with 0.27% (wt/wt) *N,N'*-methylene-bisacrylamide by the method of Laemmli (37). Fixed and dried gels were exposed to Hyperfilm Betamax (Amersham Corp., Arlington Heights, Ill.).

Marker rescue. All marker rescue experiments were done with cloned (see below) DNA fragments. The method used for transfection is based on the calcium phosphate technique of Graham and Van Der Eb (29) with modifications (48). Subconfluent monolayers of RS537 cells in 50-mm petri dishes were pretreated for 3 min at ambient temperature with 0.5 ml of a DEAE-dextran solution (200 μg/ml in PBS). After dextran was removed, cells were washed with 5 ml of MEM and covered with 5 ml of MEM supplemented with 5% fetal calf serum and antibiotics (100 units of penicillin per ml and 100 μg of streptomycin per ml). Calcium chloride (200 mM final concentration) was added to the viral DNA and linearized plasmid DNAs in HEPES-buffered saline (140 mM NaCl, 5 mM KCl, 5 mM glucose, 0.7 mM Na_2HPO_4, 20 mM HEPES [*N*-2-hydroxyethylpiperazine-*N'*-2-ethanesulfonic acid] [pH 7.08]), and coprecipitates were directly pipetted into the growth medium. The cells were allowed to incubate at 37°C for 20 h, at which time the medium was replaced by a carboxymethyl cellulose overlay (1% carboxymethyl cellulose in MEM supplemented with 5% fetal calf serum and antibiotics). Plaques developed after 3 to 4 days of incubation at 37°C or 4 to 5 days at 30°C for the controls. For each transfection experiment, the equivalent of 100 to 200 PFU of viral DNA (as assayed at 30°C) and 0.5 μg of linearized plasmid were used in a final volume of 300 μl. In these conditions, rescue was considered to be positive when 10 to 100 plaques were scored after incubation at 37°C. Control transfections with A44ts2 DNA alone produced no plaques. All marker rescue assays were performed at least in duplicate. During these experiments, we found that single-stranded viral DNA from M13 hybrids (see below) was as efficient in rescue as double-stranded replicative forms and therefore used it for some of the assays.

Cloning and sequence analysis of DNA. The HSV-1 DNA library was a gift from R. Sandri-Goldin and M. Levine; it is composed of *Eco*RI fragments from strain KOS DNA cloned into the *Eco*RI site of pBR325 (28). Plasmid pSG124, which carries the fragment *Eco*RI-A, was digested with the appropriate restriction enzymes, and subfragments were isolated by electrophoresis in low-melting-point agarose gels followed by purification through NACS-52 minicolumns (Bethesda Research Laboratories, Inc., Gaithersburg, Md.). In the same way, a *Sal*I-*Kpn*I fragment (0.545 to 0.565 map units) was isolated from purified A44ts$^+$ virion DNA. *Eco*RI-A subfragments were inserted into pBR327 (66) to generate the six plasmids pBPA2 to pBPA7 (Table 1). M13mp18 and M13mp19 (72) were used to clone the A44ts$^+$ *Sal*I-*Kpn*I fragment and fragments derived from it. The constructs pBPA1 and M13mpA44-2 (Table 1) were generated by partially digesting the parental hybrid and recircularizing the truncated forms. Ligations were performed with T4 DNA ligase, and when necessary, DNA was made blunt-ended with T4 DNA polymerase. Recipient bacterial strains were

TABLE 1. Marker rescue of A44ts2 by cloned HSV-1 DNA fragments

Plasmid or M13 construct[a]	Map coordinates of fragment or restriction site[b]	Efficiency of rescue (%)[c]
pSG1 (JK)	0.000–0.086 0.966–1.000	<0.15
pSG10 (D)	0.086–0.194	<0.15
pSG18 (F)	0.315–0.422	<0.15
pSG3 (L)	0.457–0.493	<0.15
pSG124 (A)	0.493–0.636	8
pSG22 (I)	0.636–0.724	<0.15
pSG28 (EK)	0.724–0.865	<0.15
pSG25 (H)	0.865–0.966	<0.15
pBPA1	*Eco*RI (0.493)-*Bam*HI (0.521)	<0.2
pBPA2	*Bam*HI (0.521)-*Bam*HI (0.570)	18
pBPA3	*Bam*HI (0.570)-*Bam*HI (0.575)	<0.2
pBPA4	*Bam*HI (0.575)-*Bam*HI (0.600)	<0.2
pBPA5	*Bam*HI (0.600)-*Eco*RI (0.636)	<0.2
pBPA6	*Bam*HI (0.521)-*Sal*I (0.545)	<0.1
pBPA7	*Sal*I (0.545)-*Bam*HI (0.570)	35
M13mpA44-1[d]	*Sal*I (0.545)-*Kpn*I (0.565)	52
M13mpA44-2[d]	*Acc*I (0.555)-*Kpn*I (0.565)	44
M13mpA44-3[d]	*Nco*I (0.558)-*Kpn*I (0.565)	<0.1

[a] The pSG plasmids containing the designated strain KOS *Eco*RI fragments (in parentheses) are described by Goldin et al (28). The pBPA plasmids carry subfragments of KOS *Eco*RI-A, and the M13mpA44 constructs carry the indicated A44ts$^+$ fragments.

[b] Coordinates are based on those used by Weller et al. (70).

[c] Values obtained from the number of plaques observed on monolayers cotransfected at 37°C divided by the number of plaques in parallel transfections at 30°C with an equivalent amount of A44ts2 DNA alone. Positive cotransfections gave 10 to 100 plaques, whereas no plaques were observed in negative cotransfections. All cotransfections were performed at least twice, and the values are averages.

[d] Single-stranded virion DNA was used for cotransfections.

Escherichia coli K-12 HB101 for pBR hybrids and JM105 for M13 derivatives. Bacteria were transformed by the calcium chloride procedure. Detailed protocols for these techniques are described by Maniatis et al. (39). Biohazards associated with the experiments described in this report have been examined previously by the French National Control Committee.

M13 clones were sequenced by the dideoxynucleotide-chain termination method (58). Sequence data analyses were performed by the CITI2 computer facilities in Paris. Homology searches were performed on Genbank (release 48), EMBL (release 10), and NBRF (release 11) data bases with the program of Goad and Kanehisa (27). Codon preference was analyzed with the program of Staden and McLachlan (68) with codon frequencies calculated from 12 HSV-1 coding sequences present in the Genbank data base. Amino acid sequences were aligned with the program BESTFIT (65). The nucleotide sequence of Fig. 8 has been submitted to EMBL-Genbank under the accession number M18454.

RESULTS

Phenotypic characterization of A44ts2. The mutant A44ts2 was found among the progeny of nitrosoguanidine-treated cells (Materials and Methods) infected with the A44 strain (61) of HSV-1. At 38°C, the nonpermissive temperature, plaque formation by A44ts2 was decreased by a factor of at least 10^5 relative to that at the permissive temperature, 30°C, although the parental strain A44ts$^+$ plated equally well at 30 and 38°C. Subsequently, it was noted that 37°C served equally well as the nonpermissive temperature and, for purposes of convenience, was used in some of the experiments which follow. In mixed infections of parent and mutant, no significant depression of virus yield was observed at the nonpermissive temperature, indicating that the mutation affecting A44ts2 is recessive. Infection of cell monolayers with A44ts2 at greater than 0.05 PFU per cell at the nonpermissive temperature resulted in a generalized cytopathic effect, and we were unable to directly determine a reversion frequency to ts^+. However, the absence of ts^+ plaques at lower multiplicities of infection in several trials indirectly indicated a reversion frequency of less than 10^{-5}. Single-cycle growth kinetics (Fig. 1a) showed comparable virus yields (10 to 50 PFU per cell) at 30°C for both parent and mutant, but no infectious virus was produced by A44ts2 at 38°C. The growth kinetics of A44ts2 in experiments in which permissive-to-nonpermissive temperature shifts were carried out at various times during the infectious cycle are shown in Fig. 1b. Efficient inhibition of infectious virus production was obtained in temperature shifts from 8 to 18 h postinfection. This inhibition was not due to the inactivation of completed virus, because under similar experimental conditions infectious virions of A44ts2 were not significantly more thermolabile than those of the parental strain (data not shown). The results of these experiments thus showed that the function affected in A44ts2 is not a transient early requirement but is needed throughout, or late in, the growth cycle.

We next examined the course of DNA and protein synthesis during infection. The kinetics of thymidine incorporation during infection at the nonpermissive temperature were the same for mutant and parent (data not shown), and CsCl gradient density analysis (Fig. 2) showed that for both the majority (75%) of the labeled thymidine was incorporated into material having the buoyant density of viral DNA (p = 1.728 g/cm^3). At 37°C, the electrophoretic profiles of A44ts2-induced polypeptides at early (data not shown) and late (Fig. 3) times after infection were qualitatively indistinguishable from those of A44ts$^+$; thus, the complex regulatory program of gene expression during HSV infection (67) does not appear to be disrupted in the mutant. Although no significant alterations in DNA or protein synthesis were apparent, electron microscopic examination of A44ts2-infected cells revealed that even at late times in infection, viral capsids or capsid-related structures fail to be assembled in the nucleus at the nonpermissive temperature (Fig. 4). Several hundred electron micrographs of A44ts2-infected nuclei from numerous experiments at the nonpermissive temperature were examined without the detection of such structures. On the other hand, all other alterations of the nucleus commonly seen during productive infections with wild-type HSV-1 (Fig. 4A) (13, 22, 51, 55, 59) were also seen in mutant-infected nuclei (Fig. 4B), such as marginated host chromatin, extensive electron-translucent nucleoplasm, disaggregated nucleoli, the presence of electron-dense bodies, and nuclear membrane duplication. Taken together, the above results indicate that the scope of the growth defect of A44ts2 is limited to events required for capsid assembly.

Several studies with bacteriophages (reviewed in references 19 and 20) and herpesvirus (35) have led to the notion that in those cases in which cutting of unit-length genomes from concatemers accompanies the formation of viable virus particles, capsid assembly is a necessary prerequisite to the cutting event. We (10) have previously described the use of a selective extraction procedure (32) to study the processing

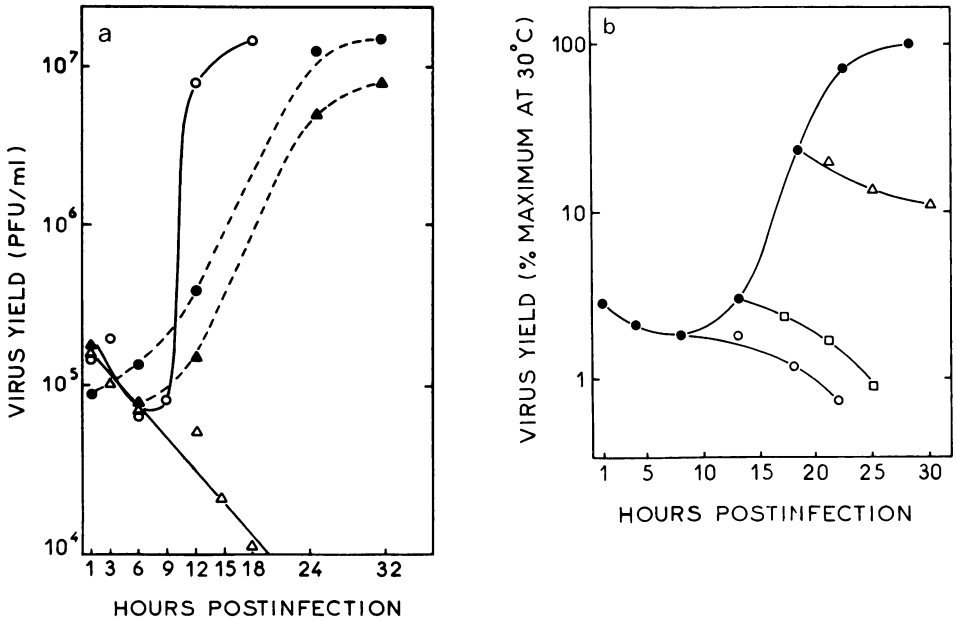

FIG. 1. Production of infectious virus by A44ts$^+$ and A44ts2 at permissive and nonpermissive temperatures. (a) Single-cycle growth kinetics. Cells were infected at 30°C (----) or 38°C (———), and virus yields were determined at the indicated times as described in Materials and Methods. Symbols: ●, ○, A44ts$^+$; ▲, △, A44ts2. (b) Effect of temperature shift-up on A44ts2 growth. Cultures infected at 30°C (●) were transferred to 38°C (○, □, △) and assayed as indicated in Materials and Methods. Temperature shifts were at 8 h (○), 13 h (□), and 18 h (△) postinfection.

of large genomes (M_r = 85 × 10^6) from intracellular, presumably concatemeric, DNA precursors during the infectious cycle of a herpesvirus. Applying the technique to the A44ts$^+$ and A44ts2 infections, we found that, in contrast to the situation with A44ts$^+$, labeled A44ts2 DNA could not be chased into the Hirt supernatant (Fig. 5) at the nonpermissive temperature, indicating a block in the production of unit-length DNA. This was supported by the finding that restriction fragments representing the physical ends of unit-length genomes were absent in intracellular A44ts2 DNA replicated at the nonpermissive temperature (data not shown).

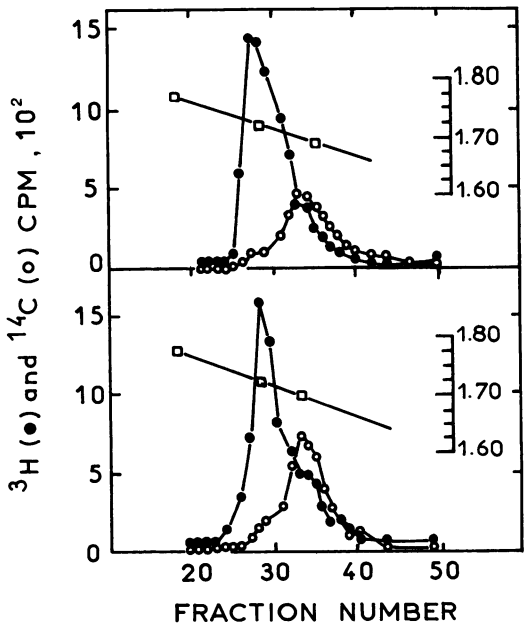

FIG. 2. Cesium chloride density gradients of DNA from cells infected at the nonpermissive temperature. Cells infected at 38°C with A44ts$^+$ (upper panel) or A44ts2 (lower panel) were labeled with [^{3}H]thymidine (●) from 6 to 9 h postinfection as described in Materials and Methods. [^{14}C]thymidine-labeled cellular DNA (○) was added as an internal density reference. The measured densities (in grams per cubic centimeter) of selected fractions are indicated (□).

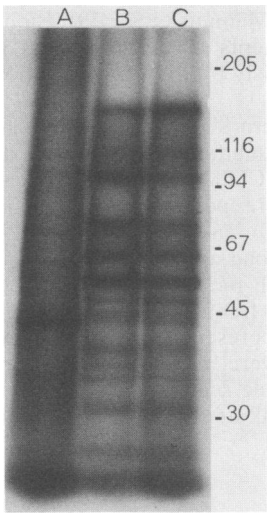

FIG. 3. Electrophoretic profiles of [^{35}S]methionine-containing polypeptides induced in cells infected at the nonpermissive temperature. Mock-infected (lane A), A44ts$^+$-infected (lane B), and A44ts2-infected (lane C) cells at 37°C were labeled from 22 to 24 h postinfection, and extracts were electrophoresed as described in Materials and Methods. The positions of molecular weight standards (×10^3) run in the same gel are indicated to the right.

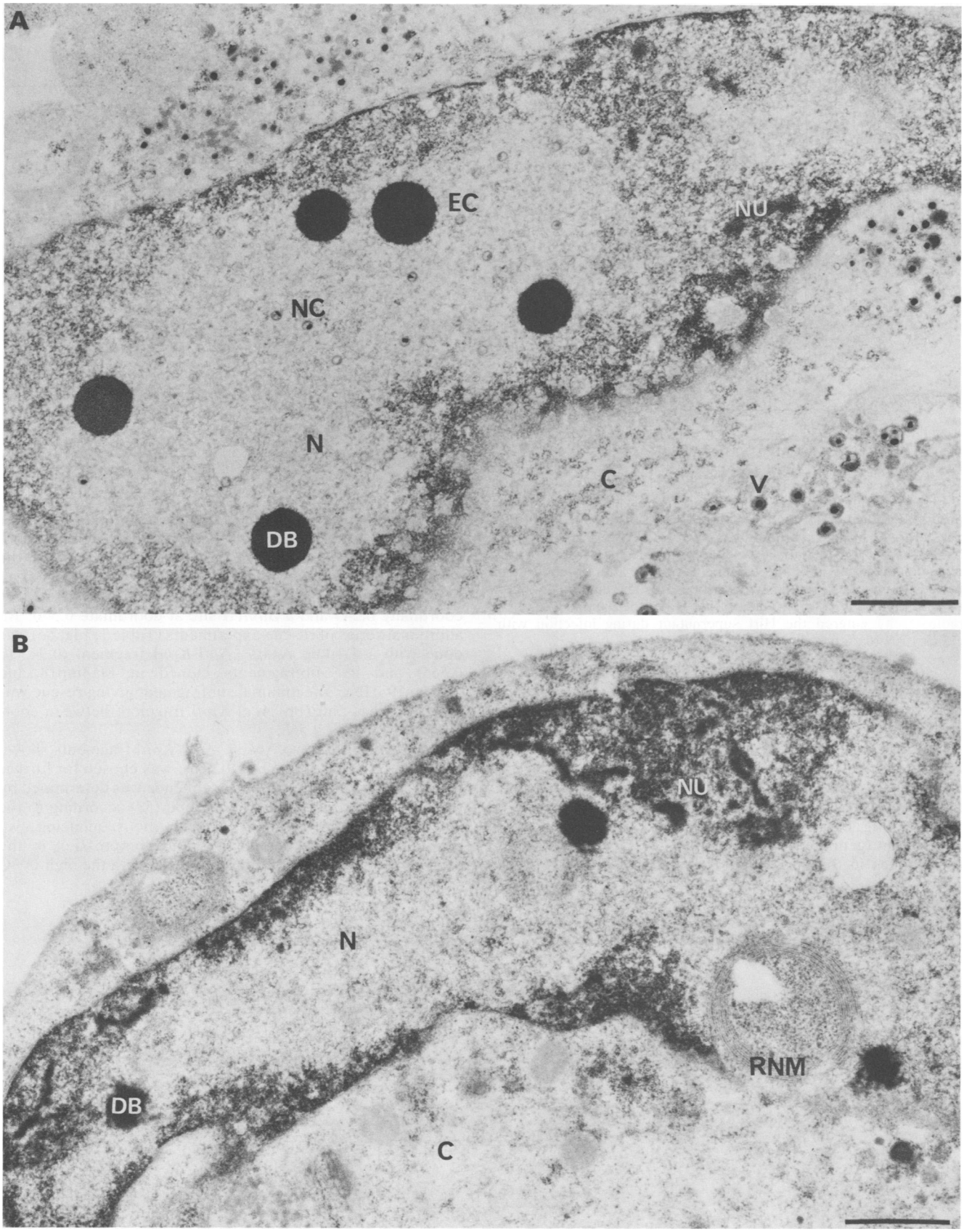

FIG. 4. Electron micrographs of infected cells late in the growth cycle at the nonpermissive temperature. Cells infected (10 PFU per cell) with A44ts$^+$ (A) or A44ts2 (B) at 37°C were processed for electron microscopy at 17 h postinfection by Epon embedding and uranyl-lead acetate staining as previously described (55). EC, Empty capsids; NC, nucleocapsids; V, enveloped virions; N, electron-translucent nucleoplasm; DB, dense bodies; NU, disaggregated nucleoli; RNM, reduplicated nuclear membrane; C, cytoplasm. Bars, 1 μm.

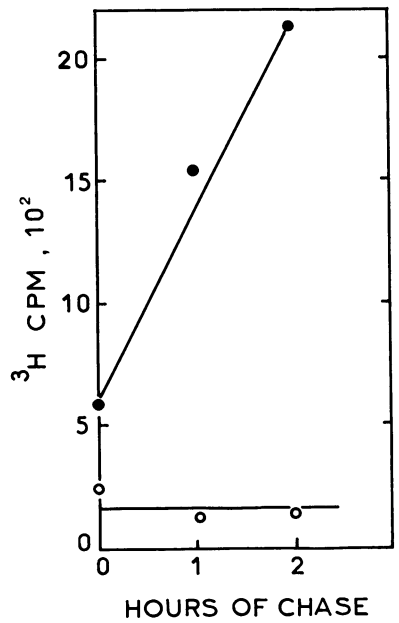

FIG. 5. Analysis by Hirt extraction of unit-length viral DNA produced at the nonpermissive temperature. Cells infected (10 PFU per cell) with A44ts$^+$ (●) or A44ts2 (○) at 37°C and labeled with [^{3}H]thymidine (5 μCi/ml) 8 to 10 h postinfection were extracted either immediately after the labeling period or after the indicated periods of chase as previously described (10). The data points refer to total radioactivity in two successive Hirt supernatants. At 30°C, radioactivity entered the Hirt supernatant during infection with either virus (data not shown).

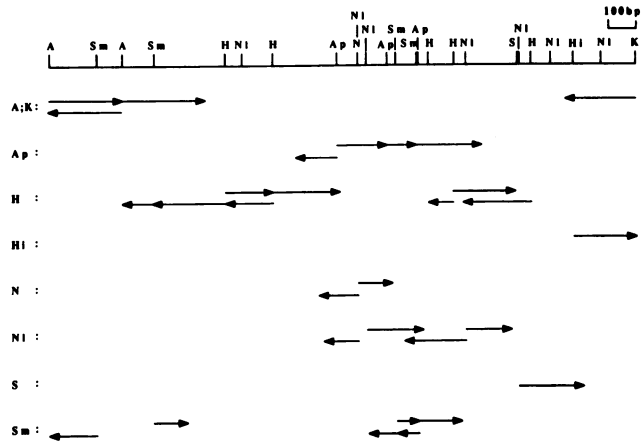

FIG. 7. Restriction map and DNA-sequencing strategy of the region between map units 0.551 and 0.565. Subfragments from the *Acc*I (0.551)-*Kpn*I (0.565) fragment of Fig. 6 produced by the indicated enzymes were subcloned into M13 vectors and sequenced by the dideoxynucleotide method. A, *Acc*I; Ap, *Apa*I; H, *Hae*II; Hi, *Hin*cII; K, *Kpn*I; N, *Nco*I; Nl, *Nla*III; S, *Sac*I; Sm, *Sma*I.

Marker rescue of the *ts*2 mutation and nucleotide sequence of the rescuing region. To locate the *ts*2 mutation in the viral genome, we used calcium phosphate coprecipitates of intact A44ts2 DNA and linearized plasmids containing strain KOS *Eco*RI fragments (28) to transfect cell monolayers at the nonpermissive temperature (37°C) as described in Materials and Methods. Of 12 plasmids from the library, 8 were tested (Table 1; Fig. 6a), and only the plasmid carrying the *Eco*RI A fragment (genome coordinates 0.493 to 0.636) gave rise to *ts*$^+$ plaques in this assay. Subfragments of *Eco*RI-A were inserted into pBR327 and used in successive marker rescue experiments to further delimit the region bearing the lesion. In one series of experiments (Table 1; Fig. 6b, c, and d), the smallest fragment allowing rescue showed this region to include 3.8 kilobase pairs (kbp) between a *Sal*I site at coordinate 0.545 and a *Bam*HI site at coordinate 0.570. An additional series of rescue experiments (Table 1; Fig. 6e) was done with a 3.1-kbp A44ts$^+$ *Sal*I-*Kpn*I fragment (0.545 to 0.565) and its subfragments cloned in M13mp18 and M13mp19. Here, the minimal subfragment giving rescue was the 1,837-base-pair (bp) *Acc*I-*Kpn*I fragment between coordinates 0.553 and 0.565.

The larger of the two A44ts$^+$ *Acc*I-*Kpn*I fragments shown in Fig. 6e, *Acc*I (0.551)-*Kpn*I (0.565), was chosen for further study. The complete nucleotide sequence was determined by the dideoxy-chain termination method (58) according to the strategy outlined in Fig. 7. During the sequencing, we encountered various degrees of band compression in the gels, a phenomenon sometimes observed with the high-G+C

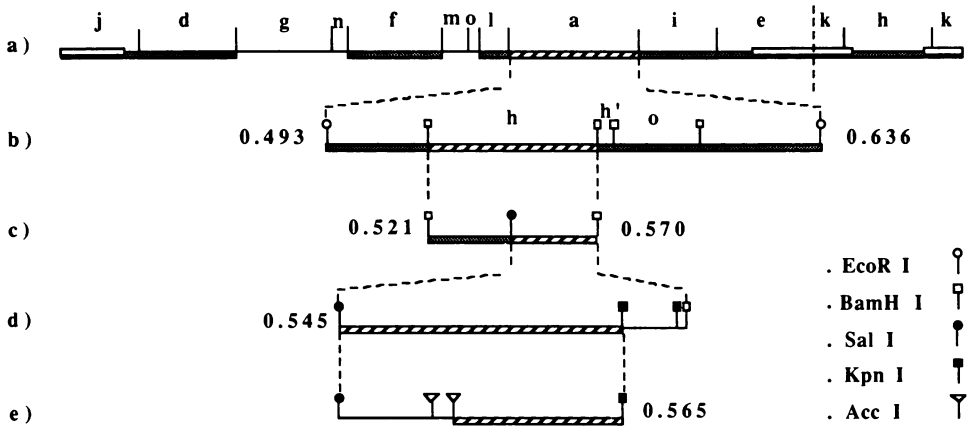

FIG. 6. Summary of marker rescue experiments to determine the location of the A44ts2 mutation. (a) *Eco*RI map of the strain KOS genome (49, 64). *Eco*RI restriction fragment profiles of strain A44ts$^+$ and strain KOS DNAs are identical, and A44ts2 DNA contains an additional *Eco*RI site in fragment I (not shown). (a to e) Restriction fragments used in marker rescue experiments (solid lines). Those rescuing the A44ts2 mutation are hatched, and those giving no rescue are stippled. Coordinates within *Eco*RI fragment A are based on 0.636 as the genomic position of the right-hand site (70), and the *Bam*HI fragments in this region (71) are indicated.

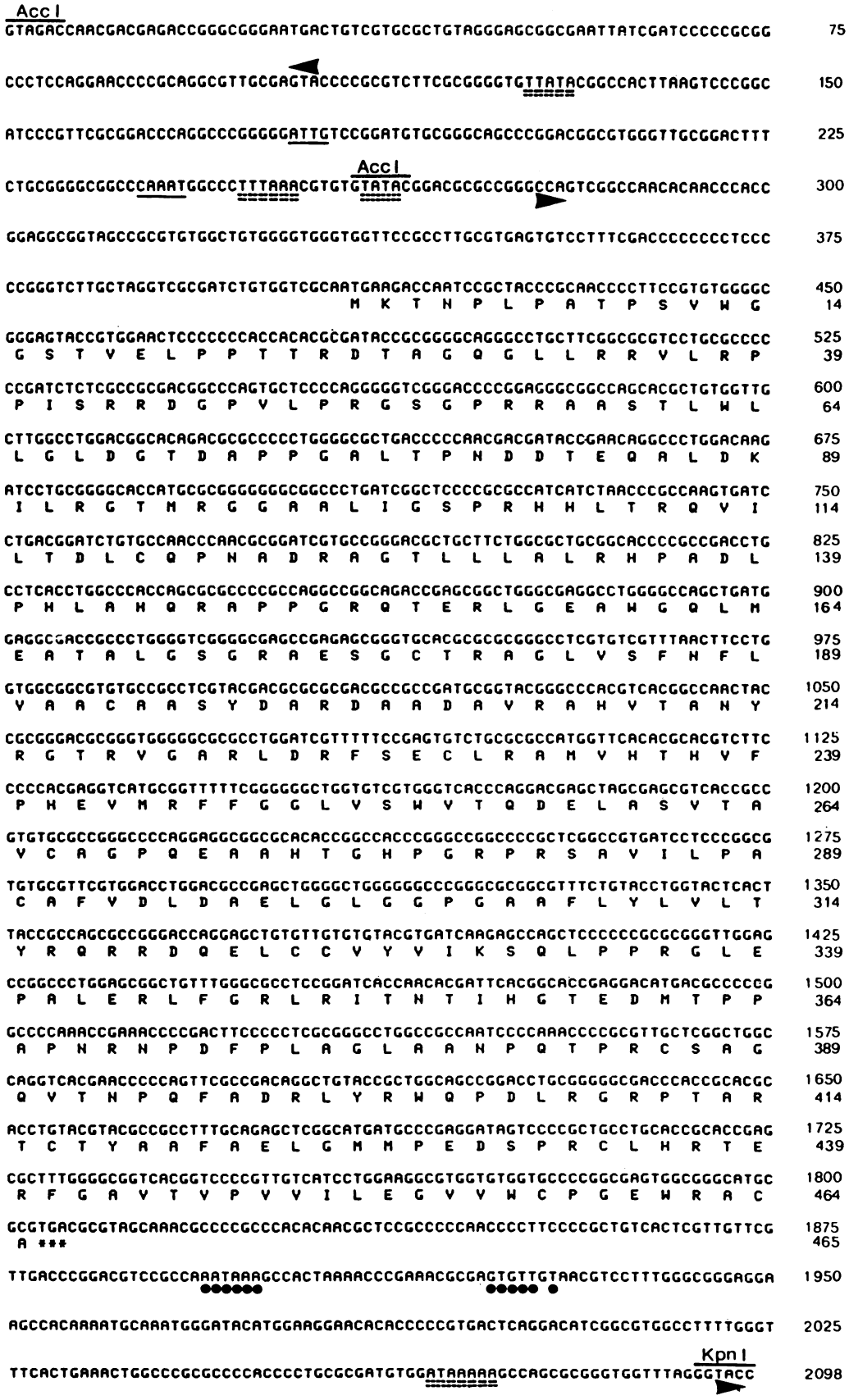

FIG. 8. Nucleotide sequence of A44ts$^+$ DNA in the genomic interval 0.551 to 0.565. The amino acid sequence of the predicted product of ORF.553 is shown in one-letter code. Also shown are putative CAAT (single underline) and TATA (double underline) transcription signals for the mRNAs mapped (2, 3) to this region (see text), as well as the locations (arrowheads) of 5′ termini for the 3.6-kb (position 116) and 1.9- and 7-kb (position 278) transcripts (M. Flanagan and E. K. Wagner, personal communication) and the cap site (position 2095) of the 5-kb transcript specifying the ribonucleotide reductase large subunit (23). Putative polyadenylation signals (47, 54) for the 1.9-kb transcript are indicated by filled circles.

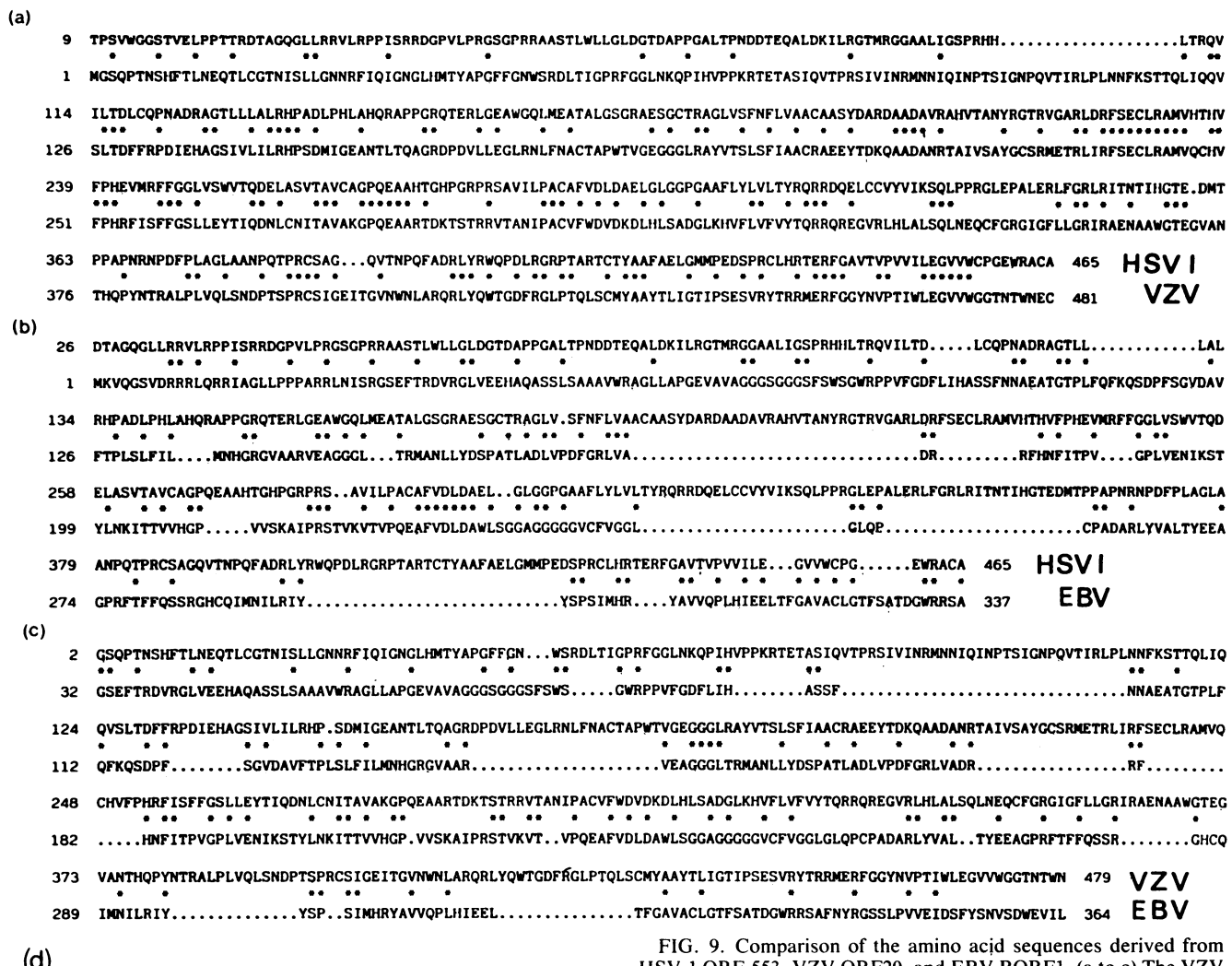

FIG. 9. Comparison of the amino acid sequences derived from HSV-1 ORF.553, VZV ORF20, and EBV BORF1. (a to c) The VZV and EBV sequences are from references 15 and 5, respectively, and the alignments were generated by the program BESTFIT (65). Asterisks denote conserved residues, and dots are gaps introduced by the program to achieve the highest scoring alignment. (d) Region of maximum shared sequence homology in the predicted products of the three ORFs. Hatched boxes designate identical residues, and open boxes identify conservative substitutions (A = I = L = V, D = E). The number to the right of each sequence shows the position of the last residue in the corresponding total sequence.

(68%) sequences of HSV (44). Although most ambiguities arising from this effect were resolvable, one recalcitrant sequence from nucleotide 1057 to nucleotide 1064 (see Fig. 8) was only decipherable with data from strain 17 communicated to us by M. A. Dalrymple and D. J. McGeoch. The three amino acids (Thr-Arg-Val) derived from this sequence therefore may not be strictly representative of strain A44.

The sequence of the 2,098-bp *Acc*I-*Kpn*I fragment (Fig. 8) was searched for probable ORFs with the aid of the codon preference program of Staden and McLachlan (68) and data from 12 HSV protein-coding regions from the Genbank data base. Among several possibilities indicated by the positions of initiation-termination codons in the six reading phases, only one extended ORF, which we refer to here as ORF.553, adhered well to HSV codon usage (data not shown). The last 100 bp of the *Acc*I-*Kpn*I fragment agree well with previously published sequences in the vicinity of the *Kpn*I site (23, 46). The sequence ATAAAAA at position 2067 is thought to belong to the promoter for a 5-kilobase (kb) RNA transcribed rightward from the middle of the *Kpn*I site (2, 23, 46). This RNA has been identified as the message for the large subunit of the viral ribonucleotide reductase (21, 53).

Three additional transcripts have also been assigned to the region including and immediately surrounding the 0.551-to-0.565 interval (2), all of which are initiated upstream of ORF.553. One, a 3.6-kb early species, is transcribed leftward, and the remaining two, 5′ coterminal late RNAs of 1.9 and 7 kb, are transcribed rightward. The positions of the 5′ ends of the three species have been determined (M. Flanagan and E. K. Wagner, personal communication) and are indicated in Fig. 8. Several putative transcriptional control signals (12) occur in this region; for the 3.6-kb RNA, sequences corresponding to TATA and CAAT boxes are present at positions −25 and −76, respectively, and two possible TATA boxes at −17 and −29, as well as a CAAT box at −39, are associated with the 1.9- and 7-kb RNAs. Downstream from ORF.553 are two polyadenylation signals, a canonical AATAAA sequence (54) 91 bp from the termi-

nation codon, and 28 bp farther along, the frequently associated consensus sequence YGTGTTY (47). Transcriptional termination in this region would give rise to an RNA of 1.6 kb, in good agreement with the 1.7 kb obtained from S1 nuclease mapping experiments (2).

ORF.553 itself extends from the ATG triplet at position 409, the context of which conforms to the preferred initiator sequences of Kozak (34), to the TGA terminator at position 1804. It thereby has the capacity to code for a 465-amino-acid protein with a predicted molecular weight of 50,175, thus fitting well with the 54,000-molecular-weight in vitro translation product of the 1.9- and 7-kb mRNAs (3). In the context of typical HSV codon usage, the in-phase triplets exhibit the position-dependent bias toward elevated G+C content already noted for various ORFs of HSV (33, 44, 45) and Epstein-Barr virus (EBV) (24); third positions are highest (86%), first positions are intermediate (73%), and second positions, which select amino acids of differing physicochemical properties, are lowest (56%).

A computer-implemented search of the EMBL and Genbank data bases failed to find nucleotide sequences with significant homology to the sequence of Fig. 8. However, in a survey of the NBRF protein data base for identical heptameric peptides, only one example was found, and this belonged to the predicted 364-amino-acid product (Fig. 9b) of the EBV BORF1 reading frame (5). As in the present case, BORF1 is located just upstream of two reading frames attributed to the viral ribonucleotide reductase (5, 24). While this work was in progress, the total nucleotide sequence of varicella-zoster virus (VZV) became available (15), and we compared the ORF.553 polypeptide with the predicted product of VZV ORF20, which also lies directly 5′ to the large subunit of VZV ribonucleotide reductase. The comparison revealed a considerably higher level of similarity than is found between the products of ORF.553 and EBV BORF1 even though the NH_2-terminal 25% of the proteins appear to have diverged to a point at which the presence of matching residues is likely to be fortuitous (Fig. 9a). A comparison of all three sequences shows that maximum sequence conservation occurs in a stretch of about 25 amino acids corresponding to the region originally detected as homologous to EBV BORF1 (Fig. 9d).

DISCUSSION

The results presented here indicate that the product of ORF.553 (UL38 [43]) functions in capsid assembly. In addition to its inability to assemble capsids at the nonpermissive temperature (Fig. 4), the mutant A44ts2 is also defective in the production of unit-length molecules from replicated viral DNA (Fig. 5). That these defects should occur together was not unexpected in view of previous findings with DNA-positive capsid-negative mutants of bacteriophages (19, 20) and the herpesvirus PrV (35) that concatemeric DNA cannot be cut to unit-length molecules in the absence of capsid formation. However, for PrV (35) and HSV-1 (62), the assembly of capsids is not a sufficient condition for cutting to take place, since some *ts* mutants which do produce capsids are nevertheless deficient in the production of unit-length DNA. Clearly, capsid assembly is only one of several requirements for DNA maturation in these viruses.

Although we have not yet identified the product of ORF.553, it is worth considering whether it could be one of the prominent structural proteins of the viral capsid. There are probably at least six of these (reviewed in references 67 and 69), of which the 155,000-molecular-weight major capsid protein (VP5 [26]; p155 [31]; NC-1 [11]) is readily ruled out on the basis of both its molecular weight and the genomic coordinates (0.2 to 0.3 [40, 50]) of its coding sequences. The most serious candidate on the basis of molecular weight would seem to be the 50,000-molecular-weight capsid protein (VP19C [31]; p50 [30]; NC-2 [11]), but studies on intertypic recombinants have placed its gene to the opposite side of the ribonucleotide reductase locus, in the coordinate region 0.58 to 0.60 (8). Lower-molecular-weight capsid components, which one could conceive of as arising from the ORF.553 product by proteolysis, for example, are the 40,000 (VP22a [26]; p40 [30]; NC-3.4 [11])-, the 32,000 (VP23 [26]; p32 [30]; NC-5 [11])-, the 25,000 (VP24 [26]; p25 [30]; NC-6 [11])-, and the 12,000 (p12 [30]; NC-7 [11])-molecular weight species. However, the genes for the 40,000- and 32,000-molecular-weight species have been mapped to the coordinate regions at 0.327 to 0.332 (52) and 0.66 to 0.76 (38), respectively. Moreover, the 12,000-molecular-weight species is a highly basic, histonelike protein (11), and no domain of the ORF.553 product appears to have such a property. By elimination, then, the only candidate remaining among these proteins would be the 25,000-molecular-weight species. Alternatively, the ORF.553 product could represent a previously unrecognized capsid component or a nonstructural protein required in the pathway of capsid assembly. Attempts are in progress to identify the ORF.553 product and to elucidate its role in capsid assembly.

Comparable ORFs are found in the published nucleotide sequences of EBV (5) and VZV (15), and it will be of interest to determine whether their products also have a role in capsid assembly. An estimate of the relatedness of these products to the ORF.553 product was obtained by computer-generated alignments of amino acid sequences (Fig. 9a and b) and by the use of an algorithm developed by Davison and Taylor (17), which takes into account the way in which identical residues are distributed in compared sequences. Their algorithm, HOMREG, scores only those sequence intervals containing at least x matching residues bounded on both sides by at least y unmatched residues, thus giving particular significance to grouped identities. It calculates both the average percentage of sequence identity within the scored intervals and the percentage of one or the other total sequences given over to these intervals. They applied the algorithm to a comparison of the VZV and EBV ORFs and suggested that the corresponding proteins of VZV ORF20 and EBV BORF1 (Fig. 9c) should be considered as "weak" homologs (i.e., 37% identity over 23% of the VZV sequence). Using their criteria ($x = 12$, $y = 5$), we found that the product of ORF.553 is a "moderate" homolog of the EBV BORF1 product (42% identity over 34% of the HSV sequence) and a "strong" homolog of the VZV ORF20 product (51% identity over 60% of the HSV sequence). The relative degree of sequence conservation between the products of ORF.553 and the VZV and EBV homologs therefore agrees with previous estimates of protein relatedness among these viruses (14–17, 25, 41–43).

In a comparison of our sequence for strain A44 with that of McGeoch et al. (42) for strain 17, there appear a number of nucleotide changes which we believe can be attributed to strain differences. There are 16 changes in the noncoding sequences—7 substitutions, 1 insertion, and a cluster of 8 deleted bases between positions 371 and 378 of the A44 sequence; none of these changes fall in the putative transcriptional control signals mentioned earlier. Within the ORF there are 12 substitutions, 8 of which occur in silent third positions and 4 of which lead to the amino acid

replacements (for A44) $V_{48}G$, $L_{313}F$, $T_{445}S$, and $C_{457}F$. A knowledge of permissible strain-dependent amino acid changes should prove useful in future attempts to define functionally important regions in this protein.

ACKNOWLEDGMENTS

We are indebted to M. Laithier and M. L. Ryhiner for expert technical assistance and to R. Sandri-Goldin and M. Levine for the gift of the KOS genomic library. We are grateful to D. J. McGeoch, P. A. Schaffer, M. Flanagan, and E. K. Wagner for communicating data prior to publication. We also thank O. Croissant for useful discussions and G. Hamon, M. Kress, A. Sarasin, and members of his laboratory for access to their computing facilities and helpful advice.

This work was supported by grants from the Centre National de la Recherche Scientifique and the Association pour la Recherche sur le Cancer, Villejuif. B.P. was a fellow of the Ministère de la Recherche et de la Technologie.

LITERATURE CITED

1. **Addison, C., F. J. Rixon, J. W. Palfreyman, M. O'Hara, and V. G. Preston.** 1984. Characterization of a herpes simplex virus type 1 mutant which has a temperature-sensitive defect in penetration of cells and assembly of capsids. Virology **138:** 246–259.
2. **Anderson, K. P., R. J. Frink, G. B. Devi, B. H. Gaylord, R. H. Costa, and E. K. Wagner.** 1981. Detailed characterization of the mRNA mapping in the *Hin*dIII fragment K region of the herpes simplex virus type 1 genome. J. Virol. **37:**1011–1027.
3. **Anderson, K. P., L. E. Holland, B. H. Gaylord, and E. K. Wagner.** 1980. Isolation and translation of mRNA encoded by a specific region of the herpes simplex virus type 1 genome. J. Virol. **33:**749–759.
4. **Atkinson, M. A., S. Barr, and M. C. Timbury.** 1978. The fine structure of cells infected with temperature-sensitive mutants of herpes simplex virus type 2. J. Gen. Virol. **40:**103–119.
5. **Baer, R., A. T. Bankier, M. D. Biggin, P. L. Deininger, P. J. Farrell, T. J. Gibson, G. Hatfull, G. S. Hudson, S. C. Satchwell, C. Séguin, P. S. Tuffnel, and B. G. Barrell.** 1984. DNA sequence and expression of the B95-8 Epstein-Barr virus genome. Nature (London) **310:**207–211.
6. **Batterson, W., D. Furlong, and B. Roizman.** 1983. Molecular genetics of herpes simplex virus. VIII. Further characterization of a temperature-sensitive mutant defective in release of viral DNA and in other stages of the viral reproductive cycle. J. Virol. **45:**397–407.
7. **Ben-Porat, T., and A. S. Kaplan.** 1985. Molecular biology of pseudorabies virus, p. 105–173. *In* B. Roizman (ed.), The herpesviruses, vol. 3. Plenum Publishing Corp., New York.
8. **Braun, D. K., W. Batterson, and B. Roizman.** 1984. Identification and genetic mapping of a herpes simplex virus capsid protein that binds DNA. J. Virol. **50:**645–648.
9. **Cabral, G. A., and P. A. Schaffer.** 1976. Electron microscopic studies of temperature-sensitive mutants of herpes simplex virus type 2. J. Virol. **18:**727–737.
10. **Cebrian, J., D. Bucchini, and P. Sheldrick.** 1983. "Endless" viral DNA in cells infected with channel catfish virus. J. Virol. **46:**405–412.
11. **Cohen, G. H., M. Ponce de Leon, H. Diggelmann, W. C. Lawrence, S. K. Vernon, and R. J. Eisenberg.** 1980. Structural analysis of the capsid polypeptides of herpes simplex virus types 1 and 2. J. Virol. **34:**521–531.
12. **Corden, J., B. Wasylyk, A. Buchwalder, P. Sassone-Corsi, C. Kedinger, and P. Chambon.** 1980. Promoter sequences of eukaryotic protein-coding genes. Science **209:**1406–1414.
13. **Dargan, D., and J. H. Subak-Sharpe.** 1983. Ultrastructural characterization of herpes simplex type 1 (strain 17) temperature sensitive mutants. J. Gen. Virol. **64:**1311–1326.
14. **Davison, A. J., and D. J. McGeoch.** 1986. Evolutionary comparisons of the S segments in the genomes of herpes simplex virus type 1 and varicella-zoster virus. J. Gen. Virol. **67:**597–611.
15. **Davison, A. J., and J. E. Scott.** 1986. The complete DNA sequence of varicella-zoster virus. J. Gen. Virol. **67:**1759–1816.
16. **Davison, A. J., and J. E. Scott.** 1986. DNA sequence of the major capsid protein gene of herpes simplex virus type 1. J. Gen. Virol. **67:**2279–2286.
17. **Davison, A. J., and P. Taylor.** 1987. Genetic relations between varicella-zoster and Epstein-Barr virus. J. Gen. Virol. **68:** 1067–1079.
18. **Dixon, R. A. F., and P. Schaffer.** 1980. Fine structure mapping and functional analysis of temperature-sensitive mutants in the gene encoding the herpes simplex type 1 immediate early protein VP175. J. Virol. **36:**189–203.
19. **Earnshaw, W. C., and S. R. Casjens.** 1980. DNA packaging by the double-stranded DNA bacteriophages. Cell **21:**319–331.
20. **Feiss, M., and A. Becker.** 1983. DNA packaging and cutting, p. 305–330. *In* R. W. Hendrix, J. W. Roberts, F. W. Stahl, and R. A. Weisberg (ed.), Lambda II. Cold Spring Harbor monograph series 13. Cold Spring Harbor Laboratory, Cold Spring Harbor, N.Y.
21. **Frame, M. C., H. S. Marsden, and B. M. Dutia.** 1985. The ribonucleotide reductase induced by herpes simplex virus type 1 involves minimally a complex of two polypeptides (136K and 38K). J. Gen. Virol. **66:**1581–1587.
22. **Friedman, A., J. E. Coward, H. S. Rosenkranz, and C. Morgan.** 1975. Electron microscopic studies on assembly of herpes simplex virus upon removal of hydroxyurea block. J. Gen. Virol. **26:**171–181.
23. **Frink, R. J., K. G. Draper, and E. K. Wagner.** 1981. Uninfected cell polymerase efficiently transcribes early but not late herpes simplex virus type 1 mRNA. Proc. Natl. Acad. Sci. USA **78:**6139–6143.
24. **Gibson, T. J., B. G. Barrell, and P. J. Farrell.** 1986. Coding content and expression of the EBV B95-8 genome in the region from base 62,248 to base 82,920. Virology **152:**136–148.
25. **Gibson, T. J., P. Stockwell, M. Ginsburg, and B. G. Barrell.** 1984. Homology between two EBV early genes and HSV ribonucleotide reductase and 38K genes. Nucleic Acids Res. **12:**5087–5098.
26. **Gibson, W., and B. Roizman.** 1972. Proteins specified by herpes simplex virus. VIII. Characterization and composition of multiple capsid forms of subtypes 1 and 2. J. Virol. **10:**1044–1052.
27. **Goad, W. B., and M. I. Kanehisa.** 1982. Pattern recognition in nucleic acid sequences. I. A general method for finding local homologies and symmetries. Nucleic Acids Res. **10:**247–263.
28. **Goldin, A. L., R. M. Sandri-Goldin, M. Levine, and J. C. Glorioso.** 1981. Cloning of herpes simplex virus type 1 sequences representing the whole genome. J. Virol. **38:**50–58.
29. **Graham, F. L., and A. J. Van Der Eb.** 1973. A new technique for the assay of infectivity of human adenovirus 5 DNA. Virology **52:**456–467.
30. **Heilman, C. J., Jr., M. Zweig, J. R. Stephenson, and B. Hampar.** 1979. Isolation of a nucleocapsid polypeptide of herpes simplex types 1 and 2 possessing immunologically type-specific and cross-reactive determinants. J. Virol. **29:**34–42.
31. **Heine, J. W., R. W. Honess, E. Cassai, and B. Roizman.** 1974. Proteins specified by herpes simplex virus. XII. The virion polypeptides of type 1 strains. J. Virol. **14:**640–651.
32. **Hirt, B.** 1967. Selective extraction of polyoma DNA from infected mouse cell cultures. J. Mol. Biol. **26:**365–369.
33. **Honess, R. W.** 1984. Herpes simplex and "the herpes complex": diverse observations and a unifying hypothesis. J. Gen. Virol. **65:**2077–2107.
34. **Kozak, M.** 1986. Point mutations define a sequence flanking the AUG initiator codon that modulates translation by eukaryotic ribosomes. Cell **44:**283–292.
35. **Ladin, B. F., M. L. Blankenship, and T. Ben-Porat.** 1980. Replication of herpesvirus DNA. V. Maturation of concatemeric DNA of pseudorabies virus to genome length is related to capsid formation. J. Virol. **33:**1151–1164.
36. **Ladin, B. F., S. Ihara, H. Hampl, and T. Ben-Porat.** 1982. Pathway of assembly of herpesvirus capsids: an analysis using DNA^+ temperature-sensitive mutants of pseudorabies virus. Virology **116:**544–561.
37. **Laemmli, U. K.** 1970. Cleavage of structural proteins during the

assembly of the head of bacteriophage T4. Nature (London) **227**:680–685.
38. **Lemaster, S., and B. Roizman.** 1980. Herpes simplex virus phosphoproteins. II. Characterization of the virion protein kinase and of the polypeptides phosphorylated in the virion. J. Virol. **35**:798–811.
39. **Maniatis, T., E. F. Fritsch, and J. Sambrook.** 1982. Molecular cloning, a laboratory manual. Cold Spring Harbor Laboratory, Cold Spring Harbor, N.Y.
40. **Marsden, H. S., N. D. Stow, V. G. Preston, M. C. Timbury, and N. M. Wilkie.** 1978. Physical mapping of herpes simplex virus-induced polypeptides. J. Virol. **28**:624–642.
41. **McGeoch, D. J.** 1987. The genome of herpes simplex virus: structure, replication and evolution. J. Cell Sci. **7**(Suppl.): 67–94.
42. **McGeoch, D. J., M. A. Dalrymple, A. J. Davison, A. Dolan, M. C. Frame, D. McNab, L. J. Perry, J. E. Scott, and P. Taylor.** 1988. The complete DNA sequence of the long unique region in the genome of herpes simplex type 1. J. Gen. Virol. **69**: 1531–1574.
43. **McGeoch, D. J., and A. J. Davison.** 1986. DNA sequence of the herpes simplex virus type 1 gene encoding glycoprotein gH, and identification of homologues in the genomes of varicella-zoster virus and Epstein-Barr virus. Nucleic Acids Res. **14**:4281–4292.
44. **McGeoch, D. J., A. Dolan, S. Donald, and D. H. K. Brauer.** 1986. Complete DNA sequence of the short repeat region of herpes simplex virus type 1. Nucleic Acids Res. **14**:1727–1745.
45. **McGeoch, D. J., H. W. Moss, D. McNab, and M. C. Frame.** 1987. DNA sequence and genetic content of the *Hin*dIII *l* region in the short unique component of the herpes simplex virus type 2 genome: identification of the gene encoding glycoprotein G, and evolutionary comparisons. J. Gen. Virol. **68**:19–38.
46. **McLauchlan, J., and J. B. Clements.** 1983. Organization of the herpes simplex virus type 1 transcription unit encoding two early proteins with molecular weight of 140,000 and 40,000. J. Gen. Virol. **64**:997–1006.
47. **McLauchlan, J., D. Gaffney, J. L. Whitton, and J. B. Clements.** 1985. The consensus sequence YGTGTTY located downstream from the AATAAA signal is required for efficient formation of mRNA 3′ termini. Nucleic Acids Res. **13**:1347–1368.
48. **Mocarski, E. S., L. E. Post, and B. Roizman.** 1980. Molecular engineering of the herpes simplex virus genome: insertion of a second L-S junction into the genome causes additional genome inversions. Cell **22**:243–255.
49. **Morse, L. S., T. G. Buchman, B. Roizman, and P. A. Schaffer.** 1977. Anatomy of herpes simplex virus DNA. IX. Apparent exclusion of some parental DNA arrangements in the generation of intertypic (HSV-1 × HSV-2) recombinants. J. Virol. **24**: 231–248.
50. **Morse, L. S., L. Pereira, B. Roizman, and P. A. Schaffer.** 1978. Anatomy of herpes simplex virus DNA. XI. Mapping of viral genes by analysis of polypeptides and functions specified by HSV-1 × HSV-2 recombinants. J. Virol. **26**:389–410.
51. **Nii, S., H. S. Rosenkranz, C. Morgan, and H. M. Rose.** 1968. Electron microscopy of herpes simplex virus. III. Effect of hydroxyurea. J. Virol. **2**:1163–1171.
52. **Preston, V. G., J. A. V. Coates, and F. J. Rixon.** 1983. Identification and characterization of a herpes simplex virus gene product required for encapsidation of virus DNA. J. Virol. **45**:1056–1064.
53. **Preston, V. G., J. W. Palfreyman, and B. M. Dutia.** 1984. Identification of a herpes virus type 1 polypeptide which is a component of the virus-induced ribonucleotide reductase. J. Gen. Virol. **65**:1457–1466.
54. **Proudfoot, N. J., and G. G. Brownlee.** 1976. 3′ Noncoding region sequences in eucaryotic mRNA. Nature (London) **263**:211–214.
55. **Puvion-Dutilleul, F., J. Pedron, M. Laithier, and P. Sheldrick.** 1982. Ultrastructural studies on the nucleus of herpes simplex type 1-infected cells. Biol. Cell **44**:249–260.
56. **Reissig, M., and A. S. Kaplan.** 1962. The morphology of noninfective pseudorabies virus produced by cells treated with 5-fluorouracil. Virology **16**:1–8.
57. **Robb, J. A., and. R. G. Martin.** 1970. Genetic analysis of simian virus 40. I. Description of microtitration and replicating techniques for virus. Virology **41**:751–760.
58. **Sanger, F., S. Nicklen, and A. R. Coulson.** 1977. DNA sequencing with chain-terminating inhibitors. Proc. Natl. Acad. Sci. USA **74**:5463–5467.
59. **Schaffer, P. A., J. P. Brunschwig, R. M. McCombs, and M. Benyesh-Melnick.** 1974. Electron microscopic studies of temperature-sensitive mutants of herpes simplex virus type 1. Virology **62**:444–457.
60. **Schaffer, P. A., V. C. Carter, and M. C. Timbury.** 1978. Collaborative complementation study of temperature-sensitive mutants of herpes simplex virus types 1 and 2. J. Virol. **27**:490–504.
61. **Sheldrick, P., M. Laithier, D. Lando, and M. L. Ryhiner.** 1973. Infectious DNA from herpes simplex virus: infectivity of double-stranded and single-stranded molecules. Proc. Natl. Acad. Sci. USA **70**:3621–3625.
62. **Sherman, G., and S. L. Bachenheimer.** 1987. DNA processing in temperature-sensitive morphogenic mutants of HSV-1. Virology **158**:427–430.
63. **Sherman, G., and S. L. Bachenheimer.** 1988. Characterization of intranuclear capsids made by ts morphogenic mutants of HSV-1. Virology **163**:471–480.
64. **Skare, J., and W. C. Summers.** 1977. Structure and function of herpesvirus genomes. II. *Eco*RI, *Xba*I, and *Hin*dIII endonuclease cleavage sites on herpes simplex type 1 DNA. Virology **76**:581–595.
65. **Smith, T. F., and M. S. Waterman.** 1981. Comparison of biosequences. Adv. Appl. Math. **2**:482–489.
66. **Soberon, X., L. Covarrubias, and F. Bolivar.** 1980. Construction and characterization of new cloning vehicles. IV. Deletion derivatives of pBR322 and pBR325. Gene **9**:287–305.
67. **Spear, P. G., and B. Roizman.** 1980. Herpes simplex viruses, p. 615–745. *In* J. Tooze (ed.), The molecular biology of tumor viruses, 2nd ed., part 2. Cold Spring Harbor monograph series **10B**, Cold Spring Harbor Laboratory, Cold Spring Harbor, N.Y.
68. **Staden, R., and A. D. McLachlan.** 1982. Codon preference and its use in identifying protein coding regions in long DNA sequences. Nucleic Acids Res. **10**:141–156.
69. **Wagner, E. K.** 1985. Individual HSV transcripts. Characterization of specific genes, p. 45–104. *In* B. Roizman (ed.), The herpesviruses, vol. 3. Plenum Publishing Corp., New York.
70. **Weller, S. K., E. P. Carmichael, D. P. Aschman, D. J. Goldstein, and P. A. Schaffer.** 1987. Genetic and phenotypic characterization of mutants in four essential genes that map to the left half of HSV-1 U_L DNA. Virology **161**:198–210.
71. **Wilkie, N. M., A. Davison, P. Chartrand, N. D. Stow, V. G. Preston, and M. C. Timbury.** 1978. Recombination in herpes simplex virus: mapping of mutations and analysis of intertypic recombinants. Cold Spring Harbor Symp. Quant. Biol. **43**: 827–840.
72. **Yanisch-Perron, C., J. Vieira, and J. Messing.** 1985. Improved M13 phage cloning vectors and host strains: nucleotide sequences of the M13mp18 and pUC19 vectors. Gene **33**:103–119.